JOURNAL OF AIRCRAFT
Vol. 40, No. 1, January–February 2003

Theoretical Solutions for Unsteady Flows Past Oscillating Flexible Airfoils Using Velocity Singularities

D. Mateescu* and M. Abdo†
McGill University, Montreal, Quebec H3A 2K6, Canada

A new method of solution is presented for the analysis of unsteady flows past oscillating airfoils. This method is based on the derivation of the singular contributions of the leading edge and ridges (points where the airfoil boundary conditions change) in the solutions of the fluid velocity and pressure coefficient. The method has been validated by comparison with the results obtained by Theodorsen and by Postel and Leppert for rigid airfoil and aileron oscillations in translation and rotation. An excellent agreement was found between the present solutions and these previous results. This method has then been used to obtain solutions for the flexural oscillations of the flexible airfoils, fitted or not with oscillating flexible ailerons, which are of interest for the aeroelastic studies. The aerodynamic stiffness, damping, and virtual (or added) mass contributions in the solutions of the unsteady pressure distribution, lift coefficient, and moment coefficient are specifically determined. An analysis of the relative magnitude of the quasi-steady and vortex shedding contributions in the aerodynamic coefficients is also presented. In all cases studied, this method led to very efficient and simple analytical solutions in closed form.

Nomenclature

$C_h(t)$ = hinge moment coefficient (positive counterclockwise), $\hat{C}_h \exp(i\omega t)$
$C_L(t)$ = unsteady lift coefficient, $\hat{C}_L \exp(i\omega t)$
$C_{La}(t)$ = aileron lift coefficient, $\hat{C}_{La} \exp(i\omega t)$
$C_m(t)$ = unsteady pitching moment coefficient (positive nose down), $\hat{C}_m \exp(i\omega t)$
$C_p(x,t)$ = unsteady pressure coefficient on the upper surface of the airfoil, $\hat{C}_p(x) \exp(i\omega t)$
$\hat{C}(k)$ = Theodorsen function[22]
$C(s)$ = $(2/\pi)\cos^{-1}\sqrt{s}$
c = airfoil chord length
cx, cy = dimensional coordinates
$\hat{D}(k)$ = $\hat{C}(k) - 1 = -iH_1^2(k)/[H_1^2(k) + iH_0^2(k)]$
$\hat{e}(x)$ = modal amplitude of flexural oscillations (positive upward), $e(x,t)/\exp(i\omega t)$
$f(s)$ = $(2/\pi)\sqrt{(1-s)s}$
$G(s,x)$ = $(2/\pi)\cosh^{-1}\sqrt{(1-x)s/(s-x)}$ for $x \in (0,s)$, $(2/\pi)\sinh^{-1}\sqrt{(1-x)s/(x-s)}$ for $x \in (s,1)$ and 0 for $x < 0$ and $x > 1$
$\tilde{G}(s,z)$ = singular contribution in $w(z)$ of a ridge situated on airfoil at $z = s$, $(2/\pi)\cosh^{-1}\sqrt{(1-z)s/(s-z)}$
g_j = $(2j-1)!/\lfloor 2^{2j}(j!)^2 \rfloor$, $g_0 = 1$
g_j = recurrence formula, $g_{j-1}(2j-1)/(2j)$
$H(s,x)$ = 1 for $x > s$ and 0 for $x < s$ $H_1(x) = 1$ for $x > 1$ and 0 for $x < 0$
$\tilde{H}(\sigma,z)$ = singular contribution in $w(z)$ of a ridge situated on the wake at $z = \sigma$, $(2/\pi)\cos^{-1}\sqrt{(1-z)\sigma/(\sigma-z)}$
$H_0^2(k)$, $H_1^2(k)$ = Hankel functions of second kind (zero and first order)
$h(t)$ = oscillatory translation along y axis (positive upwards), $\hat{h}\exp(i\omega t)$
k = reduced frequency of oscillations, $\omega c/(2U_\infty)$
s, σ = ridge positions along the x axis
U_∞ = freestream velocity
$\hat{U}(x)$ = $-i(k/c)\hat{\Gamma}_C \exp(-i2k(x-1))$
$u(x,y,t)$, $v(x,y,t)$ = perturbation velocity components along x and y axes
$\hat{u}(x,y)$, $\hat{v}(x,y)$ = reduced velocity components, $u(x,y,t)/\exp(i\omega t)$ and $v(x,y,t)/\exp(i\omega t)$ respectively
$w(z)$ = complex conjugate velocity, $\hat{u}(x,y) - j\hat{v}(x,y)$
x, y = nondimensional Cartesian coordinates, x axis along the mean position of airfoil chord
y = harmonic oscillations of the airfoil surface, $e(x,t) = \hat{e}(x)\exp(i\omega t)$ where $i = \sqrt{-1}$ and $\exp(i\omega t) = \cos\omega t + i\sin\omega t$
z = complex variable, $x + jy$ where $j = \sqrt{-1}$
$\beta(t)$ = oscillatory rotation of the aileron (positive clockwise), $\hat{\beta}\exp(i\omega t)$
$\Gamma_C(t)$ = circulation around the airfoil,

$$\int_0^1 \gamma(x,t)c\,\mathrm{d}x = \hat{\Gamma}_C \exp(i\omega t)$$

$\gamma(x,t)$ = distributed circulation along the airfoil, $\hat{\gamma}(x)\exp(i\omega t)$
$\gamma_f(x,t)$ = distributed intensity of the free vortices in the airfoil wake, $\hat{\gamma}_f(x)\exp(i\omega t)$
$\Delta C_p(x,t)$ = pressure difference coefficient across airfoil, $\Delta\hat{C}_p(x)\exp(i\omega t)$
δ_{ji} = Kronecker's symbol, 1 for $j = i$ and 0 for $j \neq i$
$\hat{\varepsilon}(x)$ = modal amplitude of aileron oscillations (positive upwards), $\varepsilon(x,t)/\exp(i\omega t)$
$\theta(t)$ = oscillatory rotation about $x = a$ (positive clockwise), $\hat{\theta}\exp(i\omega t)$
ω = radian frequency of oscillations

Superscripts

D = damping aerodynamic components
M = virtual mass aerodynamic components
Q = quasi-steady aerodynamic components
S = stiffness aerodynamic components
V = vortex-shedding aerodynamic components

Received 31 March 2002; revision received 30 August 2002; accepted for publication 6 September 2002.

*Professor in the Aeronautical Program, Aerospace Program Director, Department of Mechanical Engineering, Associate Fellow AIAA.
†Ph. D. Student, Department of Mechanical Engineering.

I. Introduction

THE steady and unsteady flows past airfoils (or wing sections) have been extensively studied during the last seven decades for their aeronautical applications. Initially, the method of conformal transformations were used to obtain steady flow solutions for particular airfoil shapes, such as the Joukowski, Kármán–Trefftz, Betz-Keune, Müller, von Mises and Carafoli-airfoils (see Refs. 1–5). The classical thin airfoil theory developed by Glauert and Birnbaum (see Refs. 1–6) established the foundation of the aerodynamics of thin airfoils of arbitrary shapes in incompressible flows, by using a modified Fourier series for the distributed vortex intensity on the chord. Based on a truncated Fourier series representation of the camberline shape (sometimes requiring a large number of terms), this classical method permitted the calculation of the aerodynamic forces and pressure distribution on the airfoil. However, as shown in Ref. 7, the Fourier series are not convenient to model aerodynamically the airfoils with discontinuities in the boundary conditions, such as the flapped airfoils. An efficient method using velocity singularities leading to simple analytical solutions in closed form has been developed by Mateescu,[8] Mateescu and Nadeau,[9] and Mateescu and Newman.[7] The methods based on velocity singularities (name introduced in Ref. 10) consist in the determination of specific singular contributions in the expression of the fluid velocity (instead of the potential), which are related to the singular points on the airfoil or wing, such as the leading edges and ridges, where the boundary conditions display sudden changes. These contributions are determined by taking into account the singular behavior of the fluid velocity at these points and satisfy all other boundary conditions, as well as the Kutta condition at the trailing edge. (They are similar to Green functions associated to these changes.) These methods were proven to be also suitable to solve problems of adaptive surfaces, such as flexible-membrane and jet-flapped airfoils.[7] More recently, methods using velocity singularities in subsonic flow have been developed for the finite span wings of arbitrary shapes[11] and for the nonlinear analysis of airfoils.[12] A method based on velocity singularities has also been developed for wing–body systems in supersonic flows.[10]

Solutions involving intensive numerical calculations have been also obtained using conformal mappings,[13–16] or using boundary element methods based on source, doublet, and vortex panels, such as those of Hess and Smith,[17] Hunt,[18] Katz and Plotkin[19] and Mateescu.[8] More recently, computational solutions have been obtained using various numerical methods for solving the Euler or Navier–Stokes equations, such as those based on finite difference or finite volume formulations (for examples see Anderson[20] and Mateescu and Stanescu[21]).

The analysis of the unsteady flows past oscillating airfoils has been mostly motivated by the efforts made to avoid or reduce undesirable unsteady effects in aeronautics, such as flutter, buffeting, and dynamic stall. Potentially beneficial effects of these unsteady flows have been also studied, such as propulsive efficiency of flapping motion, controlled periodic vortex generation, stall delay, and optimal control of unsteady forces to improve the performance of turbomachinery, helicopter rotors, and wind turbines. The foundations of the unsteady aerodynamics of oscillating airfoils have been established by Theodorsen[22] Theodorsen and Garrick,[23] Wagner,[24] Küssner,[25,26] and von Kármán and Sears,[27] who studied the unsteady flow past a thin flat plate and a trailing flat wake of vortices in incompressible flows. Further studies involving detailed unsteady flow solutions of oscillating airfoils have been performed by Postel and Leppert,[28] Fung,[29] Bisplinghoff and Ashley,[30] McCroskey,[31,32] Kemp and Homicz,[33] Basu and Hancock,[34] Dowell et al.,[35] Katz and Weihs,[36,37] and others.[38,39] Some of the recent studies used computational methods and panel methods for these unsteady aerodynamic problems; interesting analyses of unsteady flows past airfoils using panel methods are presented by Katz and Plotkin.[19]

In the aeroelastic studies, the unsteady aerodynamic analysis is performed, in conjunction with the analysis of the related structural motion, involving flexural and torsional deformations. A complete numerical approach to solve simultaneously the unsteady Euler and Navier–Stokes equations governing the unsteady flows (which involves numerous iterations for each time step) and the structural equations of motion requires a large computational effort in terms of computing time and memory, even with the present computing capabilities. For this reason, there is still a need for efficient unsteady aerodynamic solutions to be used in the aeroelasticity studies.

The main aim of this paper is to present simple and efficient aerodynamic solutions in closed form for oscillating flexible airfoils, which are obtained by a method using velocity singularities. (Previous results were mainly obtained for the case of rigid airfoil oscillations in translation and rotation.) This method is based on the derivation of specific contributions associated to the singular points on the oscillating airfoil, the leading edge, and the ridges (where the unsteady boundary conditions are changing), in the expression of the fluid velocity and unsteady pressure coefficient. These singular contributions satisfy all boundary conditions on the airfoil and outside it, including the Kutta condition at the trailing edge. As mentioned, the methods based on velocity singularities have proven to be very efficient in the analysis of steady flows past airfoils and wings (see Ref. 7–12).

II. Velocity Singularity Method for the Steady Aerodynamics of Thin Airfoils

The perturbation velocity components $u(x, y)$ and $v(x, y)$, generated by an airfoil of chord c, placed at an incidence α in a uniform stream of velocity U_∞, are harmonic functions in incompressible flow, satisfying the Laplace equation. Thus, a complex conjugate velocity $w(z) = u(x, y) - jv(x, y)$ can be defined in function of the complex variable $z = x + jy$, where x and y are nondimensional Cartesian coordinates, with the x axis along the airfoil chord and its origin at the airfoil leading edge.

The prototype problem of a flapped thin airfoil, defined by a ridge situated at $x = s$, where the airfoil slope angle suddenly changes from τ to $\tau - \beta$, due to the deflection angle β of the flap, has been solved by Mateescu and Nadeau,[9] Mateescu,[8] and Mateescu and Newman[7] using the method of velocity singularities[10] in the form

$$w(z) = A\sqrt{(1-z)/z} - \Delta v \tilde{G}(s, z) \tag{1}$$

where $\Delta v = -U_\infty \cos\alpha[\tan(\beta - \tau) + \tan\tau] \approx -\beta U_\infty$ and $A = -U_\infty(\sin\alpha - \cos\alpha\tan\tau) - \Delta v\ C(s) \approx -U_\infty(\alpha - \tau) - \Delta v\ C(s)$, and where $C(s)$ and $\tilde{G}(s, z)$ are defined in the Nomenclature. The first right-hand-side term of Eq. (1) represents the singular contribution of the airfoil leading edge (at $x = 0$), and $\tilde{G}(s, z)$ represents the singular contribution of the ridge situated at $x = s$. These singular contributions satisfy all boundary conditions on the airfoil and outside it, as well as the Kutta condition at the trailing edge. The axial perturbation velocity on the airfoil was obtained by taking the real part of Eq. (1),

$$u(x) = A\sqrt{(1-x)/x} - \Delta v G(s, x) \tag{2}$$

where $G(s, x) = \mathrm{Re}\,\{\tilde{G}(s, z)\}_{z=x}$ is also defined in the Nomenclature.

The camberline slope of a thin airfoil is expressed in general in the polynomial form

$$h'(x) = \sum_{n=0}^{N} h_n x^n$$

as in the case of NACA airfoils. The cambered airfoil was, thus, represented by a continuous distribution of elementary ridges with

$$\Delta v = \left[\frac{\mathrm{d}h'(x)}{\mathrm{d}x}\right]_{x=s} \mathrm{d}s = \sum_{n=1}^{N} n h_n s^{n-1}\,\mathrm{d}s$$

in Eq. (2), which was then integrated over the chord and led to the following expression for the pressure difference coefficient on a continuously cambered airfoil[7]:

$$\Delta C_p(x) = 4\left[\sin\alpha - \sum_{n=0}^{N} h_n \sum_{j=0}^{n} g_{n-j} x^j\right]\sqrt{\frac{1-x}{x}} \tag{3}$$

where the coefficients g_j are defined in the Nomenclature. This is a very simple expression in closed form for the thin airfoil aerodynamics, which has also proven to be very efficient for the analysis of airfoils with adaptive surfaces, such as the flexible-membrane and jet-flapped airfoils.[7]

III. Method of Solution for Unsteady Flows Past Oscillating Airfoils

Consider a thin flexible airfoil of chord c executing harmonic oscillations about its mean position situated along the axis Ox, which are defined in complex form by

$$y = e(x,t) = \hat{e}(x)\exp(i\omega t) \tag{4}$$

where the x axis along the airfoil chord is in its mean position, t is the time, and $\hat{e}(x)$ defines the modal amplitude of oscillations of the flexible airfoil. In the complex form convention used to define the oscillations, the reduced quantities marked by a caret, are complex numbers.

The boundary condition on this oscillating airfoil, $v = (\partial e/\partial t) + (U_\infty + u)(\partial e/\partial x)$, is

$$v(x,0,t) = \hat{V}(x)\exp(i\omega t), \qquad \hat{V}(x) = i\omega\hat{e}(x) + U_\infty\left(\frac{\partial\hat{e}}{\partial x}\right) \tag{5}$$

In view of the form of this boundary condition, one can introduce the reduced perturbation velocity components $\hat{u}(x,y) = u(x,y,t)/\exp(i\omega t)$ and $\hat{v}(x,y) = v(x,y,t)/\exp(i\omega t)$. Because in incompressible flows the velocity components are harmonic functions, satisfying the Laplace equation, one can introduce the complex conjugate reduced velocity $\hat{w}(z) = \hat{u}(x,y) - j\hat{v}(x,y)$, where $z = x + jy$. The boundary condition on the oscillating airfoil for $0 < x < 1$ can thus be expressed as

$$\mathrm{Im}_j\{\hat{w}(z)\}_{z=x} = -\hat{V}(x) \tag{6}$$

where the subscript j indicates an imaginary part taken with respect to the complex variable $z = x + jy$ (not with respect to i from the complex representation of the oscillatory motion).

The elementary circulation along an infinitesimal control volume around an airfoil portion of length $c\,\mathrm{d}x$ is $\mathrm{d}\Gamma = 2u(x,0,t)c\,\mathrm{d}x$, which leads to the distributed circulation on the airfoil,

$$\gamma(x,t) = \frac{\mathrm{d}\Gamma}{(c\,\mathrm{d}x)} = 2\hat{u}(x,0)\exp(i\omega t) \tag{7}$$

By integrating this relation over the chord, one obtains the unsteady circulation around the airfoil

$$\Gamma_C(t) = 2\exp(i\omega t)\int_0^1 \hat{u}(x,0)c\,\mathrm{d}x \tag{8}$$

and the reduced circulation around the airfoil, $\hat{\Gamma}_C = \Gamma_C(t)/\exp(i\omega t)$, can be expressed in the form

$$\hat{\Gamma}_C = \mathrm{Re}_j\left\{2\int_0^1 \hat{w}(z)c\,\mathrm{d}z\right\} \tag{9}$$

Because the circulation around the airfoil varies in time, at each instant in time an elementary free vortex is shed at the trailing edge, $x = 1$, through a complex process involving viscous effects. The intensity of such a free vortex shed at the trailing edge, $\mathrm{d}\Gamma_f(1,t)$, can be determined from Kelvin's circulation theorem for a material contour K, which includes the airfoil, $\mathrm{d}\Gamma_K/\mathrm{d}t = 0$, as

$$\mathrm{d}\Gamma_f(1,t) = -\left[\frac{\mathrm{d}\Gamma_C}{\mathrm{d}t}\right]\mathrm{d}t = -i\omega\hat{\Gamma}_C\exp(i\omega t)\,\mathrm{d}t \tag{10}$$

These shedding free vortices are moving downstream with the fluid flow velocity ($c\,\mathrm{d}x = U_\infty\,\mathrm{d}t$), and their distributed vortex intensity just behind the trailing edge, $\gamma_f(1,t) = \mathrm{d}\Gamma_f(1,t)/(c\,\mathrm{d}x)$ is

$$\gamma_f(1,t) = -(i\omega/U_\infty)\hat{\Gamma}_C\exp(i\omega t) \tag{11}$$

The intensity of the elementary shedding vortices remains constant in time while they are moving downstream with the fluid velocity, according to Helmholtz's circulation theorem (see Refs. 2, 4, and 5). Such a shedding vortex, situated at time t in the airfoil wake at the location $x = \sigma$, has been generated at the trailing edge at a previous time $t - \Delta t$, where the time lag $\Delta t = c(\sigma - 1)/U_\infty$ represents the time needed by this vortex to travel from the trailing edge to its present location. Thus, the intensity of the distributed vortex sheet in the wake at the location $x = \sigma$ can be calculated as

$$\gamma_f(\sigma,t) = -i(2k/c)\hat{\Gamma}_C\exp[i\omega t - i2k(\sigma - 1)] \tag{12}$$

where $k = \omega c/(2U_\infty)$ is the reduced frequency of oscillations. The reduced intensity of free wake vortices is then $\hat{\gamma}_f(\sigma) = \gamma_f(\sigma,t)/\exp(i\omega t) = 2\hat{U}(\sigma)$, where $\hat{U}(\sigma)$ is defined in Nomenclature.

Similarly to Eq. (7), one can express $\hat{u}(x,0)$ in the function of $\hat{\gamma}_f(\sigma)$ (by considering the circulation along an elementary control volume placed around a portion of the wake of length $c\,\mathrm{d}\sigma$) in the form $\hat{u}(\sigma) = \hat{\gamma}_f(\sigma)/2 = \hat{U}(\sigma)$. Thus, in addition to the boundary condition (6) on the oscillating airfoil, the complete unsteady problem formulation has to also include the following boundary conditions upstream (where $\hat{\gamma} = 0$) and downstream of the airfoil, expressed in complex form as

$$\mathrm{Re}_j\{\hat{w}(z)\}_{z=x} = H_1(x)\hat{U}(x) \tag{13}$$

for $x < 0$ and $x > 1$, where $H_1(x)$ and $\hat{U}(x)$ are defined in the Nomenclature.

Prototype Unsteady Problem Solution

To solve the problem of the oscillating airfoil, consider first the prototype unsteady problem characterized by a sudden change $\delta\hat{V}$ in the normal-to-chord velocity component on the airfoil (from $-b_0$ to $-b_0 + \delta\hat{V}$, where b_0 is a constant) and defined by the boundary conditions

$$\mathrm{Im}_j\{\delta\hat{W}(s,z)\}_{z=x} = b_0 - H(s,x)\delta\hat{V} \tag{14a}$$

$$\mathrm{Re}_j\{\delta\hat{W}(s,z)\}_{z=x} = H_1(x)\hat{U}(x) \tag{14b}$$

for $0 < x < 1$ and $x < 0$ and $x > 1$, respectively, where $H(s,x)$, $H_1(x)$, and $\hat{U}(x)$ are defined in the Nomenclature. As previously shown,[7–10,39] $\delta\hat{W}(s,z)$ displays the singularities $\sqrt{(1-z)/z}$, $\ln(s-x)$, and $\ln(\sigma - x)$ at the leading edge, $x = 0$, and at the ridges situated at $x = s$ and $x = \sigma$, where the imaginary and real parts have the changes $\delta\hat{V}$ and $\hat{U}'(\sigma)\,\mathrm{d}\sigma$, respectively.

The singular contributions associated to these ridges and satisfying the boundary conditions (14) are determined in an auxiliary complex plane defined by the conformal transformation $\chi = \sqrt{z/(1-z)}$, as shown in Refs. 7–10, leading to $\delta\hat{V}\tilde{G}(s,z)$ and $\lfloor\hat{U}'(z)\,\mathrm{d}z\rfloor_{z=\sigma}\tilde{H}(\sigma,z)$, respectively, where $\tilde{G}(s,z)$ and $\tilde{H}(\sigma,z)$ are defined in the Nomenclature. The prototype problem solution, is thus,

$$\delta\hat{W}(s,z) = -jb_0 + \delta A\sqrt{(1-z)/z} - \delta\hat{V}\tilde{G}(s,z) - (2k^2/c)\hat{\Gamma}_C\tilde{F}(z) \tag{15}$$

where

$$\tilde{F}(z) = \lim_{\sigma^*\to\infty}\int_1^{\sigma^*}\exp[-i2k(\sigma-1)]\tilde{H}(\sigma,z)\,\mathrm{d}\sigma$$

After integration by parts, $\tilde{F}(z)$ becomes

$$\tilde{F}(z) = i(c/k)\lfloor E_\infty \cos^{-1}\sqrt{1-z} + F^*(z)\rfloor \tag{16}$$

where $E_\infty = \lim_{\sigma^*\to\infty}\{\exp[-i2k(\sigma-1)]\}$ and

$$F^*(z) = \lim_{\sigma^*\to\infty}\int_1^{\sigma^*}\frac{\sqrt{(1-z)z}\exp[-i2k(\sigma-1)]}{2(\sigma-z)\sqrt{(\sigma-1)\sigma}}\,\mathrm{d}\sigma$$

Because the perturbation velocity vanishes at infinity, the unknown constant δA can now be determined from the condition $[\delta\hat{W}(s,z)]_{z\to\infty} = 0$. From the real part of this condition one obtains $E_\infty = 0$ for this indeterminate constant. [The same conclusion can also be obtained from the Riemann–Lebesque lemma on Fourier integrals when the theory of distribution is used (see Ref. 27)]. The imaginary part of this condition determines the value of the constant δA as

$$\delta A = -b_0 - \delta\hat{V}C(s) + i\hat{\Gamma}_C\frac{2k}{\pi c}\lim_{\sigma^*\to\infty}\int_1^{\sigma^*}\frac{\exp[-i2k(\sigma-1)]}{2\sqrt{(\sigma-1)\sigma}}\,\mathrm{d}\sigma \tag{17}$$

With this value of δA, Eq. (15) can be recast in the form

$$\delta\hat{W}(s,z) = -b_0\left(\sqrt{(1-z)/z} + j\right) - \delta\hat{V}\left[\tilde{G}(s,z) + \sqrt{(1-z)/z}C(s)\right] + i\hat{\Gamma}_C(2k^2/c)F(z)$$

$$F(z) = \frac{2}{\pi}\lim_{\sigma^*\to\infty}\int_1^{\sigma^*}\sqrt{\frac{(1-z)\sigma}{(\sigma-1)z}}\frac{\exp[-i2k(\sigma-1)]}{2(\sigma-z)}\,\mathrm{d}\sigma \tag{18}$$

The reduced circulation around the airfoil

$$\hat{\Gamma}_C = \mathrm{Re}\left\{2\int_0^1 \delta\hat{W}(s,z)c\,\mathrm{d}z\right\}$$

becomes now

$$\hat{\Gamma}_C = -\frac{4ic\exp(-ik/2)}{kH_1^2(k)}[1+\hat{D}(k)]\{b_0 + \delta\hat{V}[C(s)+f(s)]\} \tag{19}$$

where $f(s)$, $C(s)$, $H_1^2(k)$, and $\hat{D}(k) = \hat{C}(k) - 1$ are defined in the Nomenclature and where $\hat{C}(k)$ is Theodorsen's function.[22] (also see Refs. 23 and 28). Note that $\hat{D}(k)$ becomes zero for k tending to zero ($k\to 0$).

Reduced Pressure Coefficient

The unsteady pressure coefficient $C_p(x,t)$ on the oscillating airfoil can be obtained from the Bernoulli–Lagrange equation, and the reduced pressure coefficient, $\hat{C}_p(x) = C_p(x,t)/\exp(i\omega t)$, is

$$\hat{C}_p(x) = -(2/U_\infty)\lfloor i(k/c)\hat{\Gamma}(x) + \hat{u}(x,0)\rfloor$$

$$\hat{\Gamma}(x) = 2\int_0^x \hat{u}(x,0)c\,\mathrm{d}x \tag{20}$$

For the prototype unsteady problem, the reduced pressure coefficient is calculated as

$$\delta\hat{C}_p = -(2/U_\infty)\{i(k/c)\delta\hat{\Gamma}(x) + \mathrm{Re}_j\lfloor\delta\hat{W}(z)\rfloor_{z=x}\} \tag{21}$$

where

$$\delta\hat{\Gamma}(x) = \mathrm{Re}_j\int_0^x 2[\delta\hat{W}(z)]_{z=x}c\,\mathrm{d}x$$

One obtains, thus,

$$U_\infty\delta\hat{C}_p(s,x) = 2A\sqrt{(1-x)/x} + \delta\hat{V}[2+2ik(x-s)]G(s,x) \tag{22a}$$

$$A = \lfloor b_0 + \delta\hat{V}C(s)\rfloor\lfloor 1 + \hat{D}(k) + i2kx\rfloor + \hat{D}(k)\delta\hat{V}f(s) \tag{22b}$$

where $G(s,x) = \mathrm{Re}_j\{\tilde{G}(s,z)\}_{z=x}$ is also defined in the Nomenclature.

Complete Solution for Oscillating Airfoils

The solution of the complete unsteady flow problem of an oscillating airfoil can be obtained considering a continuous distribution of elementary ridges along the chord to model the boundary condition (6). Thus, the boundary condition change $\delta\hat{V} = [\mathrm{d}\hat{V}(x)/\mathrm{d}x]_{x=s}\,\mathrm{d}s = \hat{V}'(s)\,\mathrm{d}s$ for such an elementary ridge is introduced in the solution (22) of the prototype unsteady problem, which is then integrated with respect to s along the chord,

$$C_p(x) = \int_0^1 \delta C_p(s,x)\,\mathrm{d}s$$

In the general case of flexible airfoil oscillations, $\hat{V}(x)$, defined by boundary condition (5), is expressed in the general polynomial form

$$\hat{V}(x) = U_\infty\sum_{n=0}^{N}\hat{b}_n x^n \qquad \text{where} \qquad \hat{b}_n = b_n + i2ka_n \tag{23}$$

which leads to the following expression of the reduced pressure difference coefficient across the airfoil, $\Delta\hat{C}_p(x) = -2\hat{C}_p(x)$:

$$\Delta\hat{C}_p(x) = -4\sqrt{\frac{1-x}{x}}\sum_{n=0}^{N}\hat{b}_n\left[\sum_{j=0}^{n}g_{n-j}x^j + R_n^V + i2kR_n\right] \tag{24a}$$

$$R_n^V = \hat{D}(k)\frac{2n+1}{n+1}g_n, \qquad R_n = \frac{1}{n+1}\sum_{j=0}^{n}g_{n-j}x^{j+1} \tag{24b}$$

where R_n^V, which are proportional to $\hat{D}(k)$, represent the effect of the free shedding vortices.

To facilitate the aeroelastic applications (especially for the flexural oscillations), expression (24a) can be recast in the following form with separate pressure contributions related to the aerodynamic stiffness $P^S(x)$, aerodynamic damping $P^D(x)$, and virtual mass $P^M(x)$, which are useful in the aeroelastic studies:

$$\Delta\hat{C}_p(x) = \sqrt{\frac{1-x}{x}}[P^S(x) + i2kP^D(x) - 4k^2P^M(x)] \tag{25}$$

$$P^S(x) = -4\sum_{j=0}^{N}x^j\sum_{n=j}^{N}b_n\left(A_{nj}^Q + A_{nj}^V\right)$$

$$P^M(x) = -4\sum_{j=0}^{N}x^j\sum_{n=j}^{N}a_n\tilde{A}_{nj} \tag{26a}$$

$$P^D(x) = -4\sum_{j=0}^{N}x^j\sum_{n=j}^{N}\left(a_nA_{nj}^Q + a_nA_{nj}^V + b_n\tilde{A}_{nj}\right)$$

$$A_{nj}^Q = g_{n-j} \tag{26b}$$

$$A_{nj}^V = \hat{D}(k)g_{n-j}\left(1 + \delta_{j0}\frac{2n+1}{n+1}\right)$$

$$\tilde{A}_{nj} = \frac{g_{n-j+1}}{n+1}(1+\delta_{j1}) + (1-\delta_{j0}) \tag{26c}$$

In these expressions, A_{nj}^V, which are proportional to $\hat{D}(k)$, represent the effect of the free shedding vortices situated in the wake and are usually much smaller than the quasi-steady terms A_{nj}^Q, especially for small values of k.

Equations (24) and (25) represent two simple expressions of the general solution in closed form for the unsteady pressure difference coefficient on the airfoil, $\Delta C_p(x,t) = \Delta\hat{C}_p(x)\exp(i\omega t)$, in the general case of oscillations of flexible (or rigid) airfoils. Both unsteady solutions (24) and (25), as well as the unsteady solutions (27) of the lift and moment coefficients, reduce directly to the steady solution (3) in the limit case when k is tending to zero [because $\lim_{k\to 0}\hat{D}(k) = 0$].

The unsteady lift and pitching moment (with respect to the leading edge, positive nose down) coefficients, $C_L(t) = \hat{C}_L\exp(i\omega t)$ and $C_m(t) = \hat{C}_m\exp(i\omega t)$, can be obtained by integrating the pressure difference coefficient over the chord, thus resulting in

$$\hat{C}_L = -2\pi\sum_{n=0}^{N}\hat{b}_n g_n\frac{2n+1}{n+1}\left[1+\frac{ik}{n+2}+\hat{D}(k)\right] \tag{27a}$$

$$\hat{C}_m = -\frac{\pi}{2}\sum_{n=0}^{N}\hat{b}_n g_n\frac{2n+1}{n+1}\left[\frac{2n+2}{n+2}+\frac{i3k}{n+3}+\hat{D}(k)\right] \tag{27b}$$

These equations can also be recast in the following forms, to introduce (for the aeroelastic applications) the corresponding aerodynamic stiffness components $\hat{C}_L^S$ and $\hat{C}_m^S$, aerodynamic damping terms $\hat{C}_L^D$ and $\hat{C}_m^D$, and virtual (or added) mass components $\hat{C}_L^M$ and $\hat{C}_m^M$:

$$\hat{C}_L = \hat{C}_L^S + i2k\hat{C}_L^D - 4k^2\hat{C}_L^M, \qquad \hat{C}_m = \hat{C}_m^S + i2k\hat{C}_m^D - 4k^2\hat{C}_m^M \tag{28}$$

$$\hat{C}_L^S = -2\pi\sum_{n=0}^{N}b_n\left(L_n^Q + L_n^V\right)$$

$$\hat{C}_m^S = -\frac{\pi}{2}\sum_{n=0}^{N}b_n\left(M_n^Q + M_n^V\right) \tag{29a}$$

$$\hat{C}_L^D = -2\pi\sum_{n=0}^{N}\left(a_nL_n^Q + a_nL_n^V + b_nL_n\right)$$

$$\hat{C}_L^M = -2\pi\sum_{n=0}^{N}a_nL_n \tag{29b}$$

$$\hat{C}_m^D = -\frac{\pi}{2}\sum_{n=0}^{N}\left(a_nM_n^Q + a_nM_n^V + b_nM_n\right)$$

$$\hat{C}_m^M = -\frac{\pi}{2}\sum_{n=0}^{N}a_nM_n \tag{29c}$$

$$L_n^Q = \frac{g_n(2n+1)}{n+1}, \qquad L_n^V = \hat{D}(k)L_n^Q$$

$$L_n = \frac{L_n^Q}{2n+4} \tag{29d}$$

$$M_n^Q = \frac{2L_n^Q(n+1)}{n+2}, \qquad M_n^V = L_n^V$$

$$M_n = \frac{3L_n^Q}{2n+6} \tag{29e}$$

The terms L_n^V and M_n^V, representing the effect of the free shedding vortices situated in the wake, are usually much smaller than the quasi-steady terms L_n^Q and M_n^Q, especially for low frequency.

The unsteady lift and pitching moment coefficients can also be expressed in terms of their amplitude, A_{CL} and A_{Cm}, and phase, Ψ_{CL} and Ψ_{Cm} with respect to the airfoil oscillatory motion, as

$$C_L(t) = A_{CL}\exp(i\omega t - i\Psi_{CL})$$

$$C_m(t) = A_{Cm}\exp(i\omega t - i\Psi_{Cm}) \tag{30a}$$

$$A_{CL} = \sqrt{\left(\hat{C}_L^{\mathrm{Re}}\right)^2 + \left(\hat{C}_L^{\mathrm{Im}}\right)^2}, \qquad A_{Cm} = \sqrt{\left(\hat{C}_m^{\mathrm{Re}}\right)^2 + \left(\hat{C}_m^{\mathrm{Im}}\right)^2} \tag{30b}$$

$$\Psi_{CL} = \tan^{-1}\left(\hat{C}_L^{\mathrm{Im}}/\hat{C}_L^{\mathrm{Re}}\right), \qquad \Psi_{Cm} = \tan^{-1}\left(\hat{C}_m^{\mathrm{Im}}/\hat{C}_m^{\mathrm{Re}}\right) \tag{30c}$$

where the superscripts Re and Im denote the real and imaginary parts, such as $\hat{C}_L^{\mathrm{Re}} = \mathrm{Re}_i\{\hat{C}_L\}$ and $\hat{C}_L^{\mathrm{Im}} = \mathrm{Im}_i\{\hat{C}_L\}$. The phase lag of the aerodynamic coefficients with respect to the oscillatory motion of the airfoil is an important parameter in the aeroelastic studies.

IV. Method Validation for Oscillating Rigid Airfoils

The present method of solution has been validated by comparison with the previous results obtained by Theodorsen[22] for the lift and pitching moment coefficients and by Postel and Leppert[28] for the reduced pressure difference coefficient, in the case of rigid airfoils executing harmonic oscillations in translation, $h(t) = \hat{h}\exp(i\omega t)$, and in rotation with respect to a rotation center situated at $x = a$ on its chord, $\theta(t) = \hat{\theta}\exp(i\omega t)$. The modal amplitude of oscillations is in this case $\hat{e}(x) = \hat{h} - (x-a)\hat{\theta}$, and, hence, the coefficients b_n and a_n defining the boundary condition (5) in the form (23), where $N = 1$, become $b_0 = -\hat{\theta}$, $b_1 = 0$, $a_0 = \hat{h} + \hat{\theta}a$, and $a_1 = -\hat{\theta}$.

The reduced pressure difference coefficient and the reduced lift and pitching moment (with respect to the leading edge) coefficients are expressed in this case by Eqs. (25) and (28), where the aerodynamic stiffness, damping, and virtual mass components are

$$P^S(x) = 4\hat{\theta}\lfloor 1+\hat{D}(k)\rfloor, \qquad P^M(x) = \hat{\theta}x(1-4a-2x) - 4\hat{h}x \tag{31a}$$

$$P^D(x) = \hat{\theta}(2+8x-4a) - 4\hat{h} + \hat{D}(k)\lfloor\hat{\theta}(3-4a) - 4\hat{h}\rfloor \tag{31b}$$

$$\hat{C}_L^S = 2\pi\hat{\theta}\lfloor 1+\hat{D}(k)\rfloor, \qquad \hat{C}_L^M = 2\pi\left\lfloor\hat{\theta}\left(\tfrac{1}{8} - a/4\right) - \hat{h}/4\right\rfloor \tag{32a}$$

$$\hat{C}_L^D = 2\pi\left\{\hat{\theta}(1-a) - \hat{h} + \hat{D}(k)\left\lfloor\hat{\theta}\left(\tfrac{3}{4} - a\right) - \hat{h}\right\rfloor\right\} \tag{32b}$$

$$\hat{C}_m^S = (\pi/2)\hat{\theta}\lfloor 1+\hat{D}(k)\rfloor$$

$$\hat{C}_m^M = (\pi/2)\lfloor\hat{\theta}(9/32 - a/2) - \hat{h}/2\rfloor \tag{33a}$$

$$\hat{C}_m^D = (\pi/2)\left\{\hat{\theta}\left(\tfrac{3}{2} - a\right) - \hat{h} + \hat{D}(k)\left\lfloor\hat{\theta}\left(\tfrac{3}{4} - a\right) - \hat{h}\right\rfloor\right\} \tag{33b}$$

The pitching moment with respect to the rotation center, $x = a$, is defined as $\hat{C}_{mR} = \hat{C}_m - a\hat{C}_L$. The aerodynamic stiffness and damping components of these reduced lift and moment coefficients can also be expressed in function of their quasi-steady and vortex-shedding components (denoted by the superscripts Q and V, respectively)

$$\hat{C}_L^S = \hat{C}_L^{SQ} + \hat{C}_L^{SV}, \qquad \hat{C}_L^D = \hat{C}_L^{DQ} + \hat{C}_L^{DV}$$

$$\hat{C}_m^S = \hat{C}_m^{SQ} + \hat{C}_m^{SV}, \qquad \hat{C}_m^D = \hat{C}_m^{DQ} + \hat{C}_m^{DV} \tag{34}$$

where

$$\hat{C}_L^{SQ} = 4\hat{C}_m^{SQ} = 2\pi\hat{\theta}, \qquad \hat{C}_L^{SV} = 4\hat{C}_m^{SV} = 2\pi\hat{\theta}\hat{D}(k)$$

$$\hat{C}_L^{DQ} = 2\pi\lfloor\hat{\theta}(1-a) - \hat{h}\rfloor, \qquad \hat{C}_m^{DQ} = (\pi/2)\left\lfloor\hat{\theta}\left(\tfrac{3}{2} - a\right) - \hat{h}\right\rfloor$$

$$\hat{C}_L^{DV} = 4\hat{C}_m^{DV} = -2\pi\hat{D}(k)\left\lfloor\hat{\theta}\left(\tfrac{3}{4} - a\right) - \hat{h}\right\rfloor$$

The chordwise variations of the real and imaginary parts of the reduced pressure difference coefficient $\Delta\hat{C}_p(x)$ given by solution (31) are compared for validation in Figs. 1 and 2 with the results

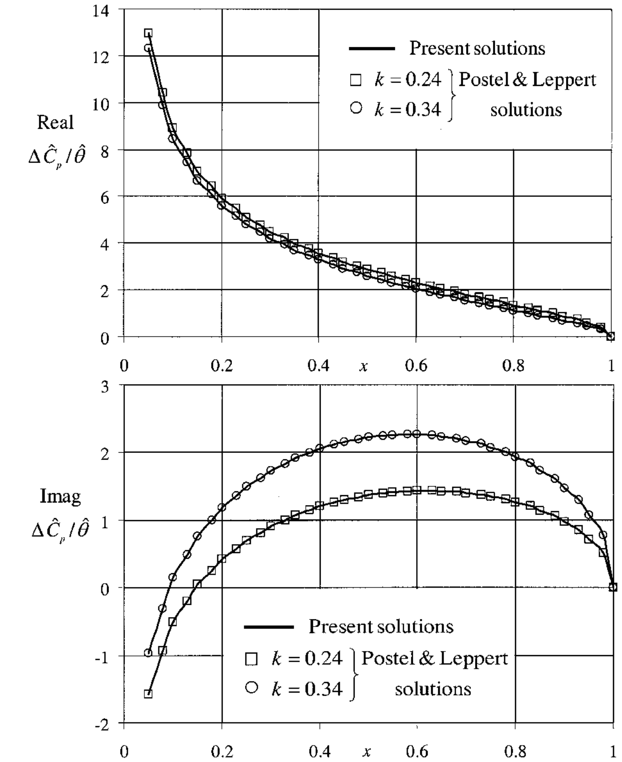

Fig. 1 Oscillatory rotation of airfoils; real and imaginary parts of the reduced pressure difference coefficient $\Delta\hat{C}_p(x)$.

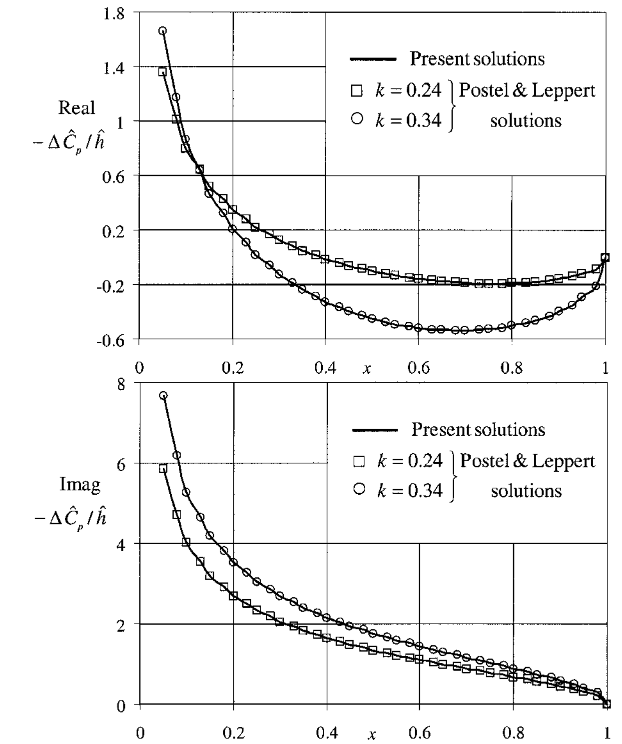

Fig. 2 Oscillatory translation of airfoils; real and imaginary parts of the reduced pressure difference coefficient $\Delta\hat{C}_p(x)$.

obtained by Postel and Leppert[28] in the cases of oscillatory rotation, $\hat{h} = 0$, and translation, $\hat{\theta} = 0$, for two values of the reduced frequency, $k = 0.24$ and $k = 0.34$. An excellent agreement can be noticed between the present solutions and Postel and Leppert[28] results in all cases.

The variation with the reduced frequency k of the real and imaginary parts of the reduced lift and pitching moment coefficients $\hat{C}_L$ and $\hat{C}_m$ given by solutions (32) and (33), in the cases of oscillatory rotation, $\hat{h} = 0$, and oscillatory translation, $\hat{\theta} = 0$, are illustrated in Figs. 3 and 4. The present solutions were found in excellent agreement with Theodorsen's results,[22] also shown.

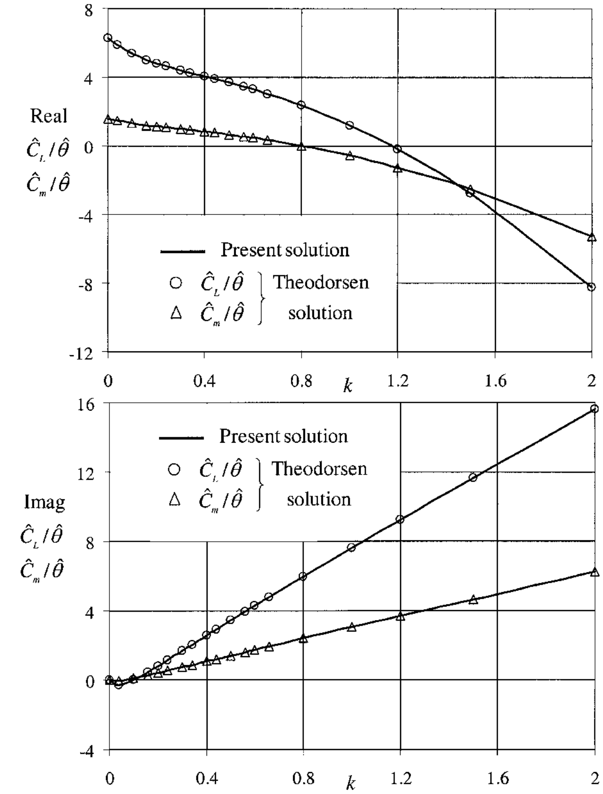

Fig. 3 Oscillatory rotation of airfoils; real and imaginary parts of the reduced lift and pitching moment coefficients $\hat{C}_L$ and $\hat{C}_m$.

Stiffness, Damping and Virtual Mass

The relative values of the aerodynamic stiffness, damping, and virtual mass contributions in the pitching moment coefficient amplitude A^S_{Cm}, $\bar{A}^D_{Cm} = (2k)A^D_{Cm}$ and $\bar{A}^M_{Cm} = (4k^2)A^M_{Cm}$ are illustrated for a rigid airfoil in oscillatory rotation in Fig. 5. Their phases with respect to the airfoil oscillations, Ψ^S_{Cm} and Ψ^D_{Cm}, are also shown. (Note that an additional 90 and 180 deg should be added to Ψ^D_{Cm} and $\Psi^M_{Cm} = 0$, respectively.)

Vortex-Shedding Effect

The variations with k of the amplitudes of the vortex-shedding and quasi-steady terms of the aerodynamic stiffness and damping contributions in the reduced lift coefficient, A^{SQ}_{CL}, A^{SV}_{CL}, $\bar{A}^{DQ}_{CL} = (2k)A^{DQ}_{CL}$, $\bar{A}^{DV}_{CL} = (2k)A^{DV}_{CL}$, are also illustrated in Fig. 5, together with the phases Ψ^{SV}_{CL} and Ψ^{DV}_{CL}, for a rigid airfoil in oscillatory rotation ($\Psi^{SQ}_{CL} = \Psi^{DQ}_{CL} = 0$). One can notice that the vortex-shedding term amplitudes are much smaller than those of the quasi-steady terms in the case of low-frequency oscillations (small k).

V. Solutions for Airfoils Executing Flexural Oscillations

Consider a flexible airfoil executing flexural oscillations, $e(x, t) = \hat{e}(x)\exp(i\omega t)$, where

$$\hat{e}(x) = \sum_{n=1}^{N} e_n x^n$$

is the modal amplitude of oscillations. In this case, the coefficients b_n and a_n become $b_n = (1 - \delta_{nN})(n+1)e_{n+1}$ and $a_n = (1 - \delta_{n0})e_n$, and the solutions for the reduced pressure, lift, and moment coefficients are given by Eqs. (24–29).

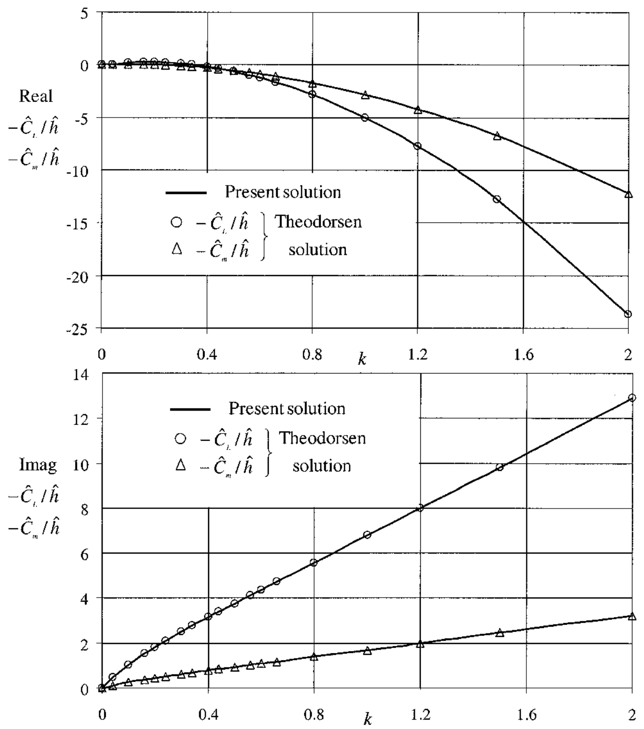

Fig. 4 Oscillatory translation of airfoils; real and imaginary parts of the reduced lift and pitching moment coefficients $\hat{C}_L$ and $\hat{C}_m$.

Parabolic Flexural Oscillations of Airfoils

As an example, consider the parabolic flexural oscillations defined as $\hat{e}(x) = e_2 x^2$, in which case $N = 2$, $b_1 = 2e_2$, $a_2 = e_2$, and the rest of the coefficients are zero. The solutions for the reduced pressure difference coefficient $\Delta\hat{C}_p(x)$ is also defined by Eq. (25), where

$$P^S(x) = e_2\lfloor 2x + 1 + 3\hat{D}(k)/2\rfloor$$

$$P^M(x) = e_2\left\lfloor x^2 + x/6 + \tfrac{1}{8}\right\rfloor \tag{35a}$$

$$P^D(x) = e_2\left\lfloor 2x^2 + x + \tfrac{3}{8} + 5\hat{D}(k)/8\right\rfloor \tag{35b}$$

and the reduced lift and moment coefficients are in this case

$$\hat{C}_L = -(\pi/2)e_2\lfloor 6 + 7ik + \hat{D}(k)(6 + 5ik) - 5k^2/4\rfloor \tag{36a}$$

$$\hat{C}_m = -(\pi/2)e_2\left\lfloor 2 + 3ik + \hat{D}(k)\left(\tfrac{3}{2} + 5ik/4\right) - 3k^2/4\right\rfloor \tag{36b}$$

For the parabolic flexural oscillations, the chordwise distributions of the real and imaginary parts of $\Delta\hat{C}_p(x)$ are shown in Fig. 6 for two values of the reduced frequency of oscillations. The variations with k of the real and imaginary parts of $\hat{C}_L$ and $\hat{C}_m$ are shown in Fig. 7.

VI. Solutions for Airfoils with Oscillating Ailerons

To determine the effect of the aileron oscillations, consider a thin airfoil of chord c at zero incidence fitted with an aileron of chord $(1 - s)c$ that executes harmonic oscillations for $s < x < 1$ defined as

$$y = \varepsilon(x, t) = \hat{\varepsilon}(x)\exp(i\omega t) \tag{37}$$

The boundary conditions on the airfoil in this case can be obtained in a similar manner as for the entire airfoil executing oscillations, resulting in, for $0 < x < 1$,

$$\mathrm{Im}_j\{\hat{w}(z)\}_{z=x} = -H(s, x)\hat{V}(x) \tag{38a}$$

and for $x < 0$, $x > 1$

$$\mathrm{Re}_j\{\hat{w}(z)\}_{z=x} = H_1(x)\hat{U}(x) \tag{38b}$$

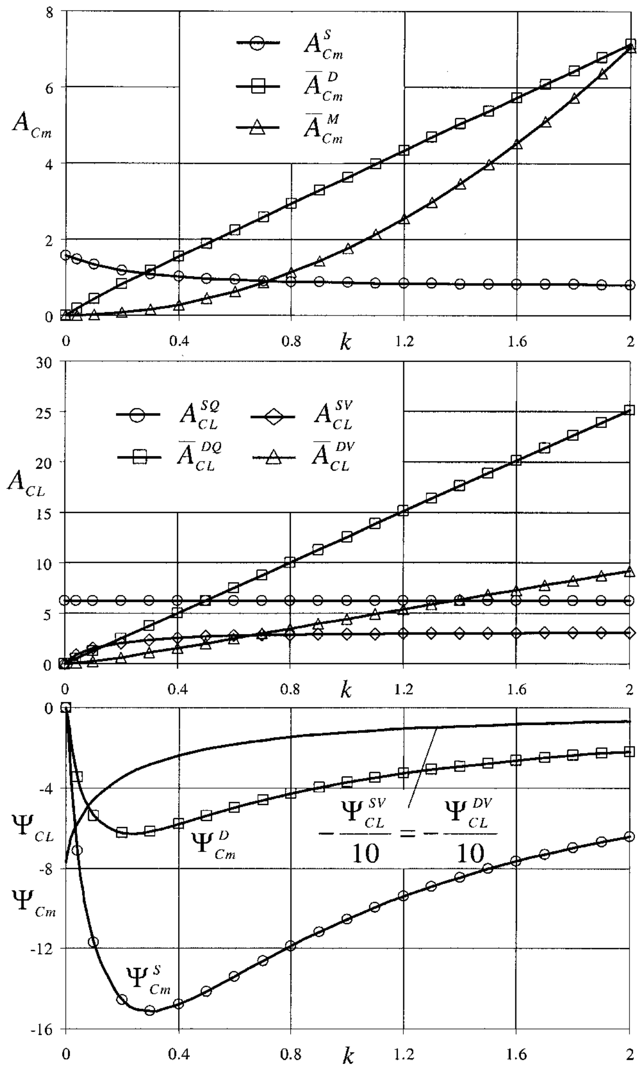

Fig. 5 Oscillatory rotation of airfoils; Aerodynamic stiffness, damping, and virtual mass contributions in the reduced pitching moment coefficient amplitude and the vortex-shedding and quasi-steady components in the reduced lift coefficient amplitude and their phases.

where $\hat{V}(x) = i\omega\hat{\varepsilon}(x) + U_\infty(\partial\hat{\varepsilon}/\partial x)$ and $H(s, x)$, $H_1(x)$, and $\hat{U}(x)$ are defined in the Nomenclature.

As shown by Eqs. (38), there is a sudden change in the boundary conditions on the airfoil at $x = s$, which is represented by the ridge contribution $\hat{V}(s)\tilde{G}(s, z)$ in the complex reduced velocity $\hat{w}(z)$. Similar to the case of oscillating airfoil, the boundary condition on the oscillating aileron can be modeled by a continuous distribution of elementary ridges, defined by the contributions $\lfloor\hat{V}'(\sigma)\,\mathrm{d}\sigma\rfloor\tilde{G}(\sigma, z)$ for $s < \sigma < 1$. Considering the solution (22) of the prototype unsteady problem for both the ridge at $x = s$ and the distribution of elementary ridges, one obtains for the reduced pressure coefficient in this case

$$U_\infty\hat{C}_p(x) = 2A\sqrt{\frac{1-x}{x}} + [2 + i2k(x - s)]\hat{V}(s)G(s, x) + \int_s^1 [2 + ik(x - \sigma)]\hat{V}'(\sigma)G(\sigma, x)\,\mathrm{d}\sigma \tag{39a}$$

$$A = \hat{V}(s)\{\lfloor 1 + \hat{D}(k) + i2kx\rfloor C(s) + \hat{D}(k)f(s)\} + \int_s^1 \hat{V}'(\sigma)\{[1 + \hat{D}(k) + i2kx]C(\sigma) + \hat{D}(k)f(\sigma)\}\,\mathrm{d}\sigma \tag{39b}$$

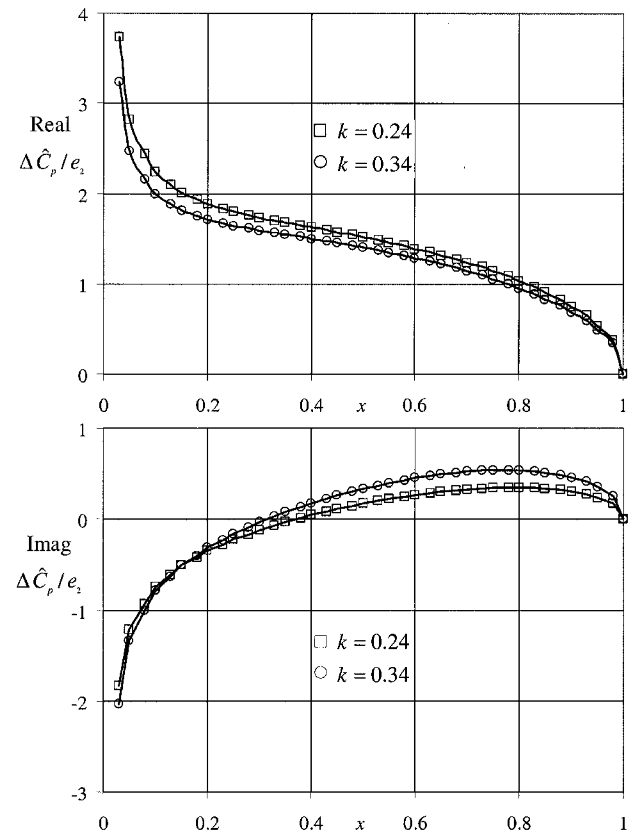

Fig. 6 Flexural oscillations of airfoils; real and imaginary parts of the reduced pressure difference coefficient $\Delta\hat{C}_p(x)$.

As in Eq. (23), the function $\hat{V}(x)$ in Eqs. (38) has the general polynomial representation

$$\hat{V}(x) = U_\infty \sum_{n=0}^{N} \hat{\beta}_n x^n, \qquad \hat{\beta}_n = \beta_n + i2k\alpha_n \tag{40}$$

After inserting this expression in Eqs. (39) and performing the integrals, one obtains the reduced pressure difference coefficient $\Delta\hat{C}_p = -2\hat{C}_p$ for the case of aileron oscillations in the form

$$\Delta\hat{C}_p(x) = -4\sqrt{\frac{1-x}{x}} \sum_{n=0}^{N} \hat{\beta}_n \left[\left(1 + \frac{i2k}{n+1}\right) \hat{P}_n^Q + \hat{P}_n^V \right]$$
$$- 4G(s,x) \sum_{n=0}^{N} \hat{\beta}_n \left[x^n + \frac{i2k(x^{n+1} - s^{n+1})}{n+1} \right] \tag{41}$$

where

$$\hat{P}_n^Q = \sum_{j=0}^{n} J_{n-j} x^{j+1}, \qquad \hat{P}_n^V = 2\hat{D}(k) J_{n+1}$$

$$J_n = \frac{\lfloor s^{n-1} f(s) + (2n-1) J_{n-1} \rfloor}{(2n)}, \qquad J_0 = C(s)$$

The reduced lift and pitching moment coefficients due to the aileron oscillations are

$$\hat{C}_L = -2\pi \sum_{n=0}^{N} \hat{\beta}_n \left\{ \sum_{j=0}^{n} J_{n-j} \left[\frac{g_j}{j+1} + \frac{i2k}{n+1} \frac{g_{j+1}}{j+2} \right] + \hat{P}_n^V + Q_n + \frac{i2k}{n+1} \left[Q_{n+1} - s^{n+1} Q_0 \right] \right\}$$

$$Q_n = \frac{f(s)}{n+1} \sum_{j=0}^{n} s^{n-j} g_j \tag{42a}$$

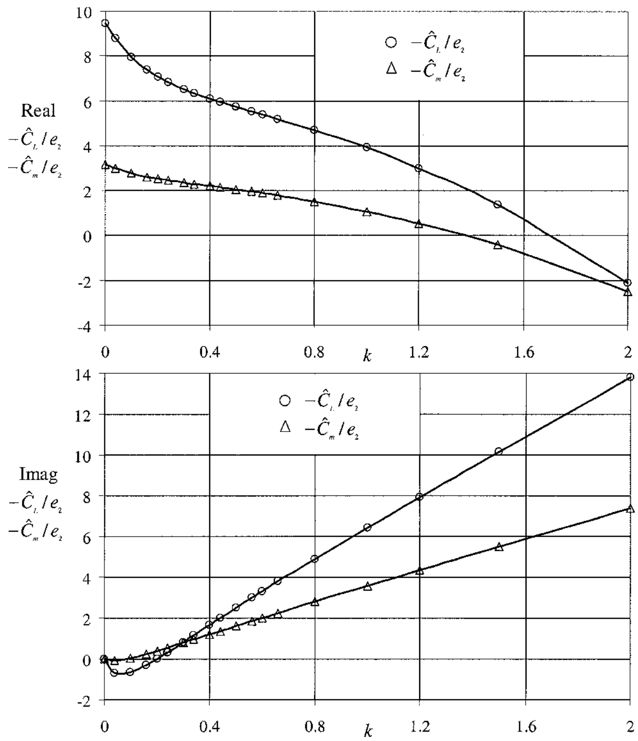

Fig. 7 Flexural oscillations of airfoils; real and imaginary parts of the reduced lift and pitching moment coefficients $\hat{C}_L$ and $\hat{C}_m$.

$$\hat{C}_m = -2\pi \sum_{n=0}^{N} \hat{\beta}_n \left\{ \sum_{j=0}^{n} J_{n-j} \left[\frac{g_{j+1}}{j+2} + \frac{i2k}{n+1} \frac{g_{j+2}}{j+3} \right] + \frac{\hat{P}_n^V}{4} + Q_{n+1} + \frac{i2k}{n+1} \left[Q_{n+2} - s^{n+1} Q_1 \right] \right\} \tag{42b}$$

The unsteady lift coefficient of the aileron and the hinge moment, $C_{La}(t) = \hat{C}_{La} \exp(i\omega t)$ and $C_h(t) = \hat{C}_h \exp(i\omega t)$, are obtained by integrating $\Delta\hat{C}_p(x)$ over the aileron in the form

$$\hat{C}_{La} = -\frac{2\pi}{1-s} \sum_{n=0}^{N} \hat{\beta}_n \left\{ \sum_{j=0}^{n} J_{n-j} \left(\bar{L}_j + \frac{i2k}{n+1} \bar{L}_{j+1} \right) + \hat{P}_n^V L_0 + \bar{Q}_n + \frac{i2k}{n+1} \left[\bar{Q}_{n+1} - s^{n+1} \bar{Q}_0 \right] \right\}$$

$$\bar{Q}_n = \frac{f(s)}{n+1} \sum_{j=0}^{n} s^{n-j} J_j \tag{43a}$$

$$\hat{C}_h = -\frac{2\pi}{(1-s)^2} \sum_{n=0}^{N} \hat{\beta}_n \left\{ \sum_{j=0}^{n} J_{n-j} \left(\bar{L}_{j+1} + \frac{i2k}{n+1} \bar{L}_{j+2} \right) + \hat{P}_n^V \bar{L}_1 + \bar{Q}_{n+1} + \frac{i2k}{n+1} \left[\bar{Q}_{n+2} - s^{n+1} \bar{Q}_1 \right] \right\}$$

$$\bar{L}_j = \frac{\lfloor J_j - s^j f(s) \rfloor}{(j+1)} \tag{43b}$$

Method Validation for a Rigid Aileron Executing Oscillatory Rotation

In the case of a rigid aileron executing oscillatory rotations about the hinge at $x = s$, the modal amplitude of oscillations is $\hat{\varepsilon}(x) = -(x-s)\hat{\beta}$, and, hence, the coefficients β_n and α_n defining the boundary condition (38) in the form (40), where $N = 1$,

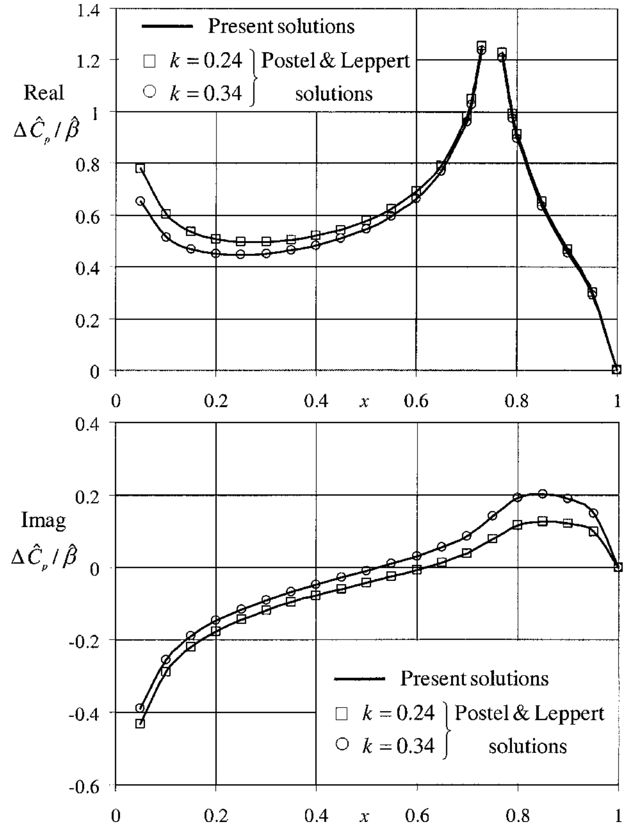

Fig. 8 Oscillatory rotation of ailerons; real and imaginary parts of the reduced pressure difference coefficient $\Delta\hat{C}_p(x)$.

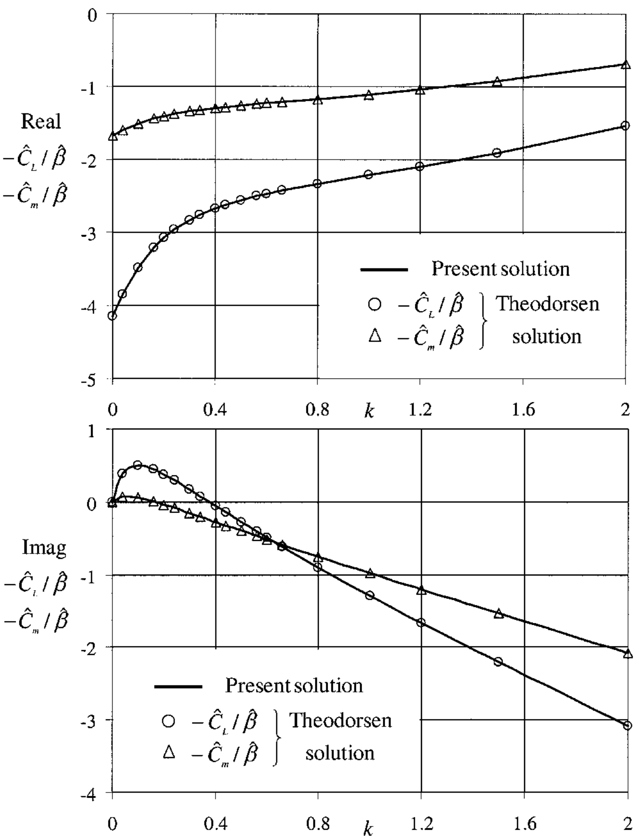

Fig. 9 Oscillatory rotation of ailerons; real and imaginary parts of the reduced lift and pitching moment coefficients $\hat{C}_L$ and $\hat{C}_m$.

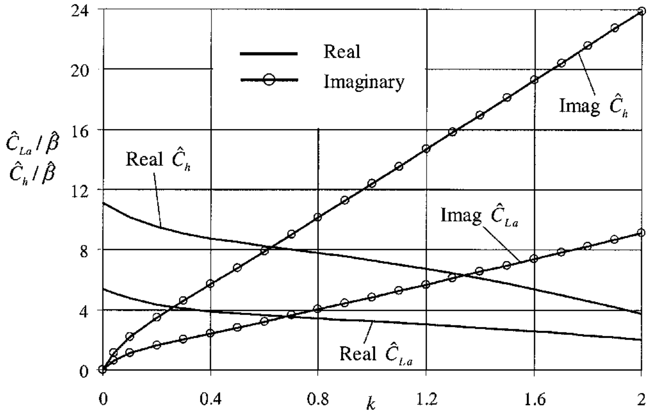

Fig. 10 Oscillatory rotation of ailerons; real and imaginary parts of the reduced aileron lift and hinge moment coefficients $\hat{C}_{La}$ and $\hat{C}_h$.

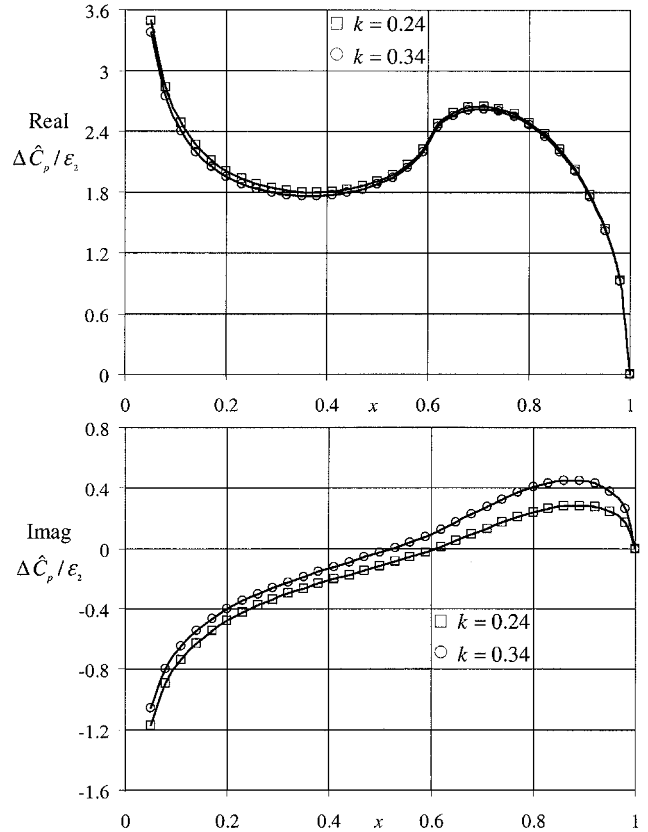

Fig. 11 Flexural oscillations of ailerons; real and imaginary parts of the reduced pressure difference coefficient $\Delta\hat{C}_p(x)$.

become $\beta_0 = -\hat{\beta}$, $\beta_1 = 0$, $\alpha_0 = \hat{\beta}s$, and $\alpha_1 = -\hat{\beta}$. Then $\Delta\hat{C}_p(x)$, $\hat{C}_L$, $\hat{C}_m$, $\hat{C}_{La}$, and $\hat{C}_h$ are determined from Eqs. (41–43).

The chordwise variations of the real and imaginary parts of $\Delta\hat{C}_p(x)$ are shown in Fig. 8 for $s = 0.75$ and two values of the reduced frequency of oscillations, $k = 0.24$ and $k = 0.34$.

The variations with k of the real and imaginary parts of the reduced lift and pitching moment coefficients $\hat{C}_L$ and $\hat{C}_m$, and of the reduced aileron lift and hinge moment coefficients $\hat{C}_{La}$ and $\hat{C}_h$ are shown in Figs. 9 and 10 for $s = 0.7$. The present solutions were found in excellent agreement with the results obtained by Theodorsen[22] and by Postel and Leppert,[28] also shown in these figures.

Aileron Executing Flexural Oscillations

Consider a flexible airfoil executing flexural oscillations, $\varepsilon(x, t) = \hat{\varepsilon}(x)\exp(i\omega t)$, where

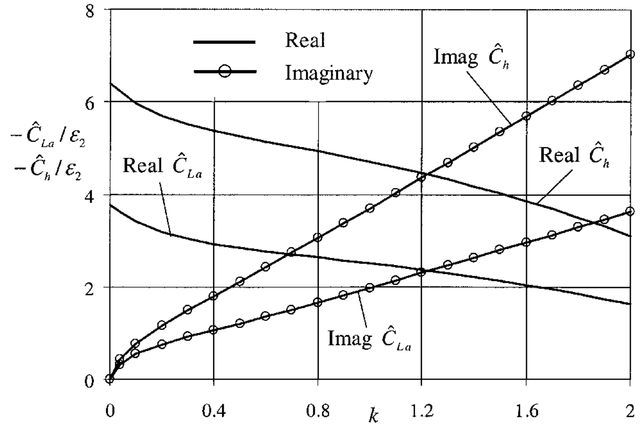

Fig. 12 Flexural oscillations of ailerons; real and imaginary parts of the reduced aileron lift and hinge moment coefficients $\hat{C}_{La}$ and $\hat{C}_h$.

$$\hat{\varepsilon}(x) = \sum_{n=0}^{N} \varepsilon_n (x - s)^n$$

is the modal amplitude of oscillations, which leads to the corresponding values of the coefficients β_n and α_n, and the solutions for the reduced pressure, lift, and moment coefficients are obtained from Eqs. (41–43).

Parabolic Flexural Oscillations of Ailerons

As an example, consider the parabolic flexural oscillations defined as $\hat{\varepsilon}(x) = \varepsilon_2(x - s)^2$, in which case $N = 2$, $\beta_0 = -2\varepsilon_2 s$, $\alpha_0 = \varepsilon_2 s^2$, $\beta_1 = 2\varepsilon_2$, $\alpha_1 = -2\varepsilon_2 s$, $\beta_2 = 0$, and $\alpha_2 = \varepsilon_2$.

For the parabolic flexural oscillations, the chordwise distributions of the real and imaginary parts of the reduced pressure difference coefficient $\Delta\hat{C}_p(x)$ are shown in Fig. 11 for $s = 0.6$ and two values of k. The variations with k of the real and imaginary parts of the reduced aileron lift and hinge moment coefficients $\hat{C}_{La}$ and $\hat{C}_h$ are shown in Fig. 12 for $s = 0.6$.

VII. Conclusions

A new method of solution has been presented for the analysis of unsteady flows past oscillating airfoils. The method is based on the determination of the singular contributions of the leading edge and ridges (points where the airfoil boundary conditions change) in the expression of the reduced velocity and pressure coefficient. This led to very efficient and simple theoretical solutions in closed form. These unsteady flow solutions lead directly to the steady flow solutions in the limit case when the frequency of oscillations tends to zero.

The method has been validated for the case of rigid airfoil and aileron oscillations in translation and rotation, by comparison with the results obtained by Theodorsen[22] for the lift and moment coefficients and by Postel and Leppert[28] for the reduced pressure difference coefficient. An excellent agreement was found between the present solutions and these previous results.

Then, the present method was used to derive efficient theoretical solutions, also in closed form, for the case of flexural oscillations of flexible airfoils, fitted or not with oscillating flexible ailerons, which are of interest for the aeroelastic studies in the aeronautical applications.

To facilitate the aeroelastic applications, the aerodynamic stiffness, damping, and virtual (or added) mass contributions in the solutions of the unsteady pressure distribution, lift, and moment coefficients are specifically determined. An analysis of the relative magnitude of the quasi-steady and vortex-shedding contributions in the aerodynamic coefficients is also presented.

Acknowledgments

The support of the Natural Sciences and Engineering Research Council of Canada is gratefully acknowledged.

References

[1] Anderson, J. D., *Fundamentals of Aerodynamics*, 2nd ed., McGraw–Hill, New York, 1991, Chap. 4.

[2] Carafoli, E., *Tragflügeltheorie*, VebVerlag, Berlin, 1954, Chap. 5.

[3] Milne-Thomson, L. M., *Theoretical Aerodynamics*, Dover, New York, 1966, Chap. 6–8.

[4] Kuethe, A. M., and Chow, C.-Y., *Foundations of Aerodynamics*, Wiley, New York, 1986, Chap. 5.

[5] Thwaites, B., *Incompressible Aerodynamics*, Oxford Univ. Press, Oxford, 1960, Chap. 4.

[6] Glauert, H., *The Elements of Aerofoil and Airscrew Theory*, Cambridge Univ. Press, England, UK, 1959, Chap. 7, 9.

[7] Mateescu, D., and Newman, B. G., "Analysis of Flexible-Membrane and Jet-Flapped Airfoils Using Velocity Singularities," *Journal of Aircraft*, Vol. 28, No. 11, 1991, pp. 789–795.

[8] Mateescu, D., "A Hybrid Panel Method for Aerofoil Aerodynamics," *Boundary Element XII*, Vol. 2, Springer-Verlag, Berlin, 1990, pp. 3–14.

[9] Mateescu, D., and Nadeau, Y., "A Nonlinear Analytical Solution for Airfoils in Irrotational Flows," *Proceedings of 3rd International Congress of Fluid Mechanics*, Vol. 4, 1990, pp. 1421–1423.

[10] Mateescu, D., "Wing and Conical Body of Arbitrary Cross Section in Supersonic Flow," *Journal of Aircraft*, Vol. 24, No. 4, 1987, pp. 239–247.

[11] Mateescu, D., Seytre, J. F., and Berhe, A. M., "Aerodynamic Solutions for Finite-Span Wings of Arbitary Shapes," *Applied Aerodynamics Conference, 41st AIAA Aerospace Sciences Meeting and Exhibit*, Reno, Nevada, AIAA 2003-1098, Jan. 2003.

[12] Mateescu, D., "Steady and Unsteady Flow Solutions Using Velocity Singularities for Fixed and Oscillating Airfoils and Wings," *Computational Methods and Experimental Measurements X*, Computational Mechanics, Southampton, New York, 2001, pp. 3–12.

[13] Sells, C. C. L. "Plane Subcritical Flow Past a Lifting Aerofoil," *Proceedings of the Royal Society of London, Series A: Mathematical and Physical Sciences*, Vol. 308, 1968, pp. 377–401.

[14] Halsey, N. D., "Potential Flow Analysis of Multielement Airfoils Using Conformal Mapping," *AIAA Journal*, Vol. 17, No. 12, 1979, pp. 1281–1288.

[15] Ives, D. C., "A Modern Look at Conformal Mapping Including Multiple Connected Regions," *AIAA Journal*, Vol. 14, No. 8, 1976, pp. 1006–1011.

[16] Bauer, F., Garabedian, P., and Korn, D., *Supercritical Wing Sections*, Springer, Berlin, 1972, Chap. 3.

[17] Hess, J. L., and Smith, A. M. O., "Calculation of Potential Flow About Arbitrary Bodies," *Progress in Aerospace Sciences*, Vol. 8, Pergamon Press, New York, 1967, pp. 1–138.

[18] Hunt, B., *Numerical Methods in Applied Fluid Dynamics*, Academic Press, London, 1980, pp. 49–136.

[19] Katz, J., and Plotkin, A., *Low Speed Aerodynamics*, McGraw–Hill, New York, 1991, Chap. 5, 6, 9–11, 13.

[20] Anderson, E., *Computational Fluid Dynamics*, McGraw–Hill, New York, 1985, Chap. 6.

[21] Mateescu, D., and Stanescu, D., "A Biased Flux Method for Solving the Euler Equations in Subsonic, Transonic and Supersonic Flows," *Computational Methods and Experimental Measurements VII*, Computational Mechanics, Southampton, New York, 1995, pp. 327–335.

[22] Theodorsen, T., "General Theory of Aerodynamic Instability and the Mechanism of Flutter," NACA TR 496, 1935.

[23] Theodorsen, T., and Garrick, I. E., "Nonstationary Flow About a Wing–Aileron–Tab Combination Including Aerodynamic Balance," NACA Rept. 736, 1942.

[24] Wagner, H., "Dynamischer Auftrieb von Tragflügeln," *Zeitschrift für Angewandte Mathematik und Mechanik*, Vol. 5, 1925, p. 17.

[25] Küssner, H. G., "Zusammenfassender Bericht über den instationären Auftrieb von Flügeln," *Luftfahrtforschung*, Vol. 13, 1936, p. 410.

[26] Küssner, H. G., "Nonstationary Theory of Airfoils of Finite Thickness in Incompressible Flow," *AGARD Manual on Aeroelasticity*, Part 2, 1960, Chap. 5.

[27] von Kármán, T., and Sears, W. R., "Airfoil Theory for Nonuniform Motion," *Journal of Aeronautical Sciences*, Vol. 5, 1938, pp. 370–390.

[28] Postel, E. E., and Leppert, E. L., "Theoretical Pressure Distributions for a Thin Airfoil Oscillating in Incompressible Flow," *Journal of Aeronautical Sciences*, Vol. 15, 1948, pp. 486–492.

[29] Fung, Y. C., *An Introduction to the Theory of Aeroelasticity*, Dover, New York, 1993, pp. 381–462.

[30] Bisplinghoff, R. I., and Ashley, H., *Principles of Aeroelasticity*, Dover, New York, 1962, Chap. 4.

[31] McCroskey, W. J., "Inviscid Flow Field of an Unsteady Airfoil," *AIAA Journal*, Vol. 11, 1973, pp. 1130–1137.

[32] McCroskey, W. J., "Unsteady Airfoils," *Annual Review of Fluid Mechanics*, Palo Alto, CA, Vol. 14, 1982, pp. 285–311.

[33]Kemp, N. H., and Homicz, G., "Approximate Unsteady Thin Airfoil Theory for Subsonic Flow," *AIAA Journal*, Vol. 14, No. 8, 1976, pp. 1083–1089.

[34]Basu, B. C., and Hancock, G. J., "The Unsteady Motion of a Two-Dimensional Airfoil in Incompressible Inviscid Flow," *Journal of Fluid Mechanics*, Vol. 87, Pt. 1, July 1978, pp. 159–178.

[35]Dowell, E. H., Bland, S. R., and Williams, M. H., "Linear/Nonlinear Behavior in Unsteady Transonic Aerodynamics," *22nd AIAA Structural Dynamics and Material Conference*, Atlanta, AIAA Paper 81-0643, 1981.

[36]Katz, J., and Weihs, D. "Large Amplitude Unsteady Motion of a Flexible Slender Propulsor," *Journal of Fluid Mechanics*, Vol. 90, Pt. 4, Feb. 1979, pp. 713–723.

[37]Katz, J., and Weihs, D. "Wake Rollup and the Kutta Condition for Airfoils Oscillating at High Frequency," *AIAA Journal*, Vol. 19, No. 12, 1981, pp. 1604–1606.

[38]Anderson, J. M., Streitlien, K., Barrett, D. S., and Triantafyllou, M. S., "Oscillating Foils of High Propulsive Efficiency, *Journal of Fluid Mechanics*, Vol. 360, April 1998, pp. 41–72.

[39]Carafoli, E., Mateescu, D., and Nastase, A., *Wing Theory in Supersonic Flow*, Pergamon, Oxford, 1969, Chap. 2.